Exploring seasonal accumulation bias in a west central Greenland ice core with observed and reanalyzed data

Stacy E. PORTER,[1,2] Ellen MOSLEY-THOMPSON[1,2]

[1]*Byrd Polar and Climate Research Center, The Ohio State University, Columbus, OH, USA*
E-mail: porter.573@osu.edu
[2]*Atmospheric Sciences Program, Department of Geography, The Ohio State University, Columbus, OH, USA*

ABSTRACT. The seasonality of accumulation in west central Greenland is investigated to determine whether a summer bias exists in a multi-century ice core recovered from Crawford Point (CP). Such a bias would negatively affect the ice core's potential for reconstructing the history of winter circulation patterns including the North Atlantic Oscillation. An automatic weather station (AWS) installed at the CP site in 1995 records sub-daily surface heights and affords a unique opportunity to assess the seasonal distribution of accumulation and test the performance of five gridded reanalysis datasets and a regional climate model. Simulated accumulation compares remarkably well with in situ measurements from both the AWS and CP ice core, demonstrating their potential to accurately represent accumulation in this region. Seasonal accumulation exhibits no summer maximum, indicating that any concurrent precipitation maximum is likely offset by melt and/or sublimation effects. The lack of a strong seasonal accumulation bias implies that the CP ice core is well suited for future investigations of the history of winter circulation patterns.

KEYWORDS: accumulation, ice core, ice-sheet mass balance

INTRODUCTION

Ice cores provide crucial and often unique records of climate variability for regions with sparse observations and for the pre-instrumental period. The thicknesses of individual annual layers and the annual averages of the oxygen isotopic ratio ($\delta^{18}O$) originating from the precipitation preserved in glaciers and ice sheets provide essential proxy records of annual net accumulation and temperature, respectively. However, these annually resolved records may contain seasonal biases reflecting the distribution of precipitation throughout the year. For example, if a drill site receives considerably more summer than winter precipitation then the annually averaged $\delta^{18}O$ value and the net annual accumulation may be more representative of summer conditions. Hence, knowledge of potential seasonal biases is essential for accurate interpretation and utilization of the proxy records.

Ice-core-derived paleo-proxy data are commonly used to study the past behavior of large-scale circulations and teleconnection patterns such as the North Atlantic Oscillation (NAO). The NAO signal is best preserved in ice-core-derived accumulation records from west central Greenland (Appenzeller and others, 1998; Mosley-Thompson and others, 2005; Calder and others, 2008). The NAO is a dominant wintertime phenomenon that heavily influences the position and intensity of the North Atlantic storm track. Winter precipitation over the Greenland ice sheet (GrIS) is governed by cyclones associated with this storm track, while summer synoptic patterns include generally weaker cyclones over Baffin Bay to the west (Schuenemann and others, 2009). Merz and others (2013) found that annual synoptic fields governing accumulation in west central Greenland resemble the winter fields, suggesting that winter variability is likely captured in the annual signal. However, they also noted that the seasonal variability captured depends strongly on the seasonal contribution of accumulation, which varies under different climate states. This study focuses on the seasonal distribution of accumulation, but seasonal variability is also important when examining annually resolved proxy data, especially for regions where one season tends to dominate the annual variability.

Previous modeling and reanalysis studies suggest that the large sub-region of west central Greenland typically receives more precipitation in summer than in winter (Chen and others, 1997; Bromwich and others, 1999). These studies are supported by sparse observations from meteorological stations in Greenland located primarily along the coast, where steep and complex topographical gradients strongly influence the spatial patterns of precipitation. Precipitation gauges at these stations have difficulty distinguishing between solid and liquid precipitation and also suffer from severe under-catchment issues, especially in windy conditions, which are more prevalent in winter. Although adjustments are made to overcome some of these difficulties (Aðalgeirsdóttir and others, 2009), the precipitation data may not fully represent the actual precipitation along the coast and are even less likely to represent precipitation further inland over the ice sheet. Moreover, reanalysis datasets assimilate these station data into models and interpolate them over Greenland to a coarse resolution grid, which may not be able to capture the spatially complex precipitation dynamics. Thus, the summer precipitation maximum reported by previous studies for the entirety of west central Greenland may primarily reflect coastal trends.

Given the recent reconstruction of a 241 year annually resolved proxy history from the 2007 Crawford Point (CP) ice core in west central Greenland (Porter, 2013), it is crucial to examine the seasonal distribution of precipitation and accumulation in the vicinity of the drill site. Fortunately, sub-hourly surface height data from a nearby (within 3 km) automatic weather station (AWS), installed in May 1995, make this assessment possible. The in situ ice-core-derived accumulation and AWS surface height measurements are compared with precipitation from four coastal stations and

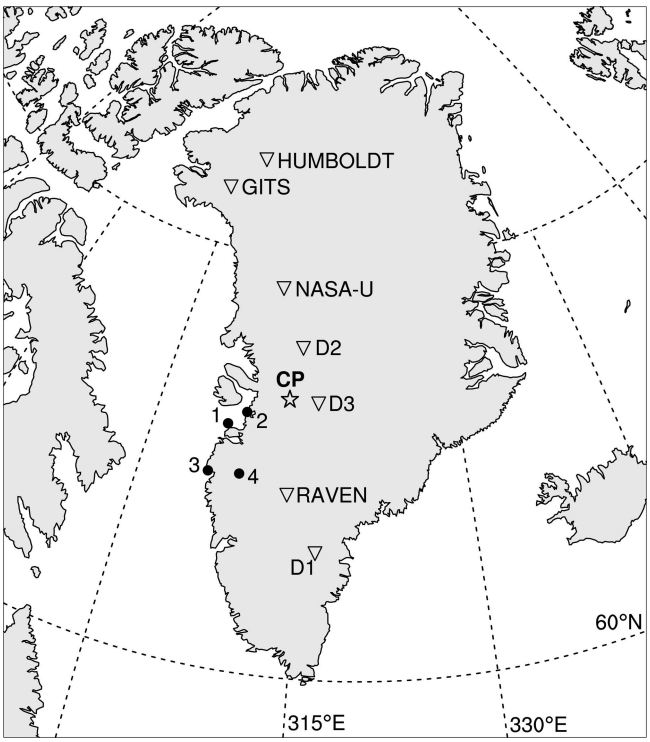

Fig. 1. Map of Greenland showing locations of the CP ice core (star), multi-century cores drilled by previous Program for Arctic Regional Climate Assessment (PARCA)/CReSiS projects (inverted triangles) and meteorological stations measuring precipitation (circles). Numbers refer to stations: 1. Aasiaat; 2. Ilulissat; 3. Sisimiut; 4. Kangerlussuaq.

with accumulation at the CP site derived from five reanalysis datasets and a regional model at the CP site. Based upon the agreement between the reanalyzed and modeled accumulation and the AWS observations, the simulated data extend the analysis of accumulation seasonality prior to installation of the AWS.

DATA AND METHODS

In 2007 a long (152 m) multi-century ice core was drilled at CP (69.90° N, 47.00° W; ~2000 m a.s.l.) as part of a Center for Remote Sensing of Ice Sheets (CReSIS) field campaign (Fig. 1). CP is located in the upstream region of the Jakobshavn Isbræ drainage basin. The CP core was dated back to AD 1766 using well-preserved seasonal variations in both $\delta^{18}O$ and the concentration of insoluble dust particles. Oxygen isotopic fractionation depends on temperature, so $\delta^{18}O$ serves as a proxy for temperature where minima represent winter and maxima represent summer. Annual layers are delineated by $\delta^{18}O$ minima, winter to winter, which approximately represent a calendar year (Fig. 2a), and the thickness between $\delta^{18}O$ minima represents the net annual accumulation (A_n). To account for the thinning of annual layers with depth due to snow and firn compaction and densification, the annual layer thicknesses were converted to water equivalent (w.e.) using a density model constructed from densities measured on the core as it was drilled (Fig. 2b). No adjustments were made for thinning due to ice flow, given the short length of the core (152 m) relative to the total ice thickness (~2000 m). Thus, the CP ice core

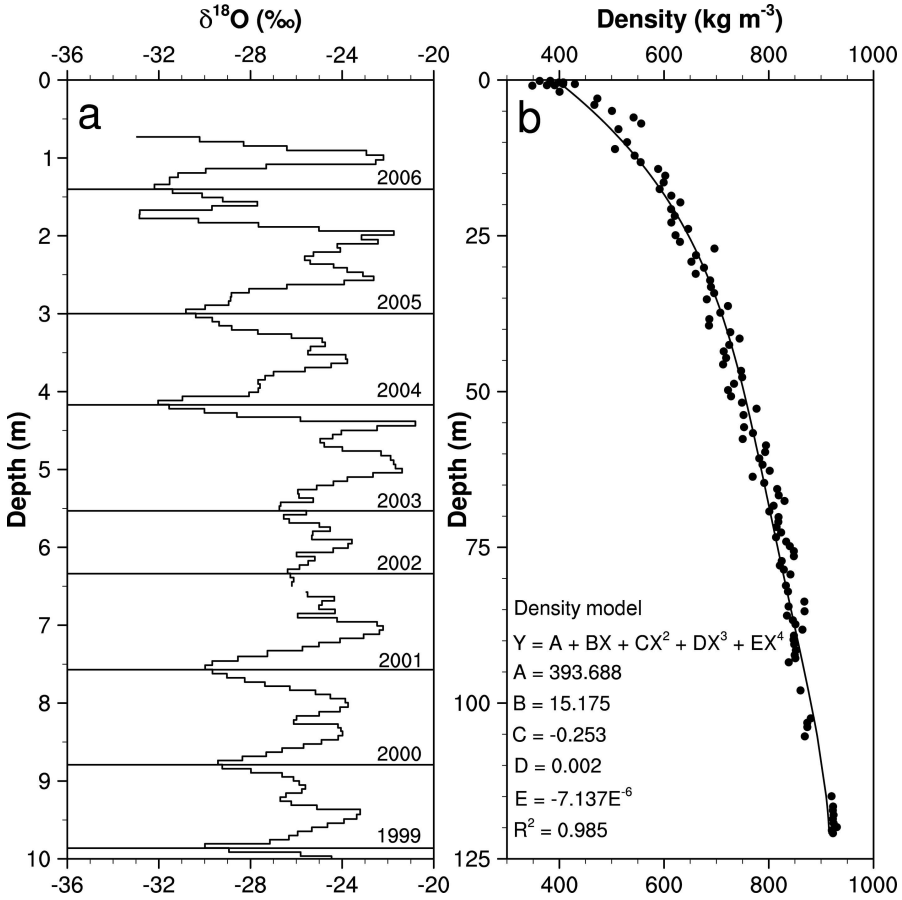

Fig. 2. (a) $\delta^{18}O$ measurements for each sample in a 10 m section of the CP ice core illustrating delineation of years and determination of annual layer thicknesses. (b) Density measurements (circles) and model (line) for the core.

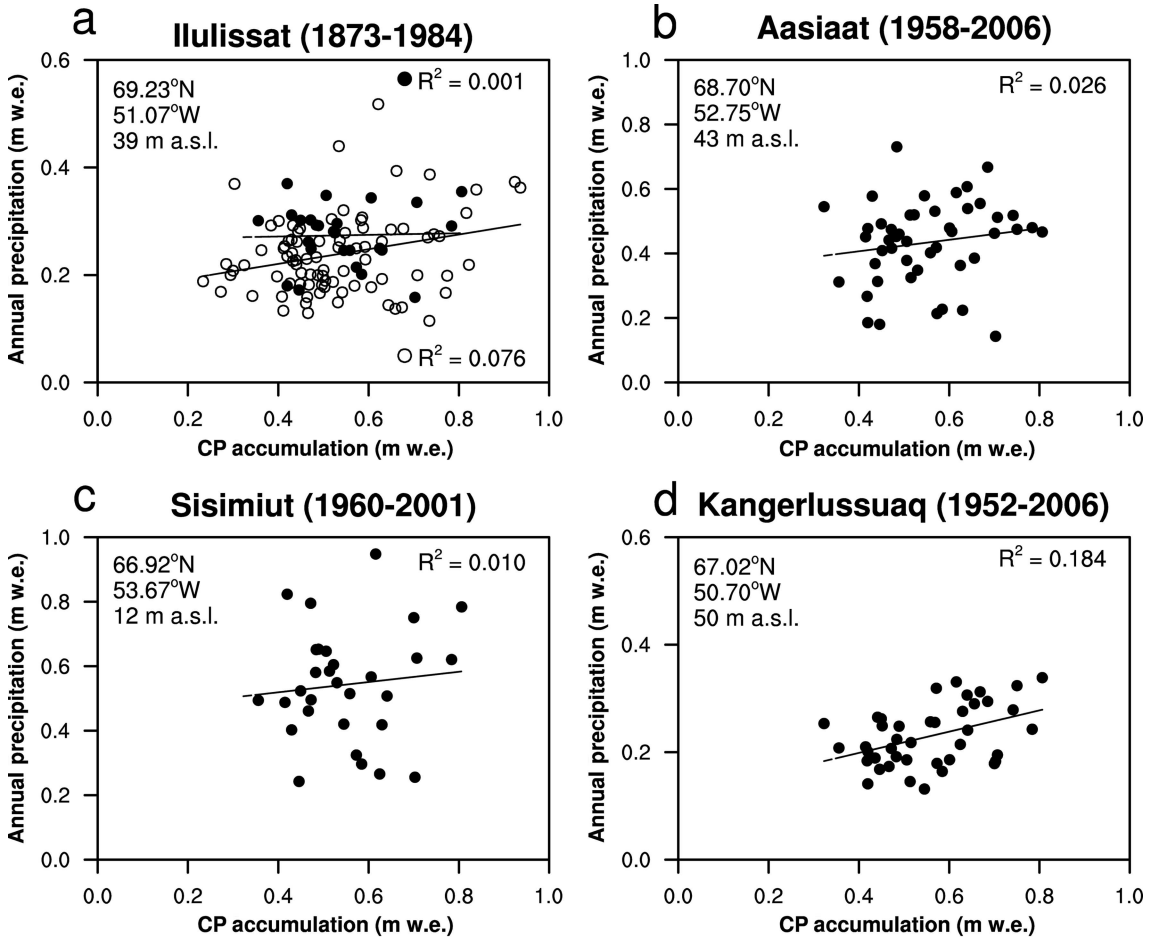

Fig. 3. Scatter plots for CP annual accumulation and annual station precipitation after 1960 (open circles for Ilulissat represent 1874–1959); only the relationship with Kangerlussuaq is significant at the 99% confidence level.

yields an annually resolved record of net accumulation (A_n). Extraction of robust sub-annual accumulation information from the CP ice core is not possible. However, the AWS observations and simulated accumulation provide an opportunity to investigate sub-annual timescales to determine whether a seasonal bias is present.

NASA's Program for Arctic Regional Climate Assessment (PARCA) was developed to understand climatological and glaciological changes in the surface mass balance of the GrIS by employing remote-sensing technologies and a comprehensive network of AWSs and ice cores (Mosley-Thompson and others, 2001; Steffen and Box, 2001; Thomas and PARCA, 2001). During the PARCA campaign, an AWS was installed at CP (69.88° N, 46.99° W) in May 1995 and has recorded sub-hourly measurements of air and snow temperature, wind speed and direction, relative humidity, pressure, shortwave radiation and changes in snow height. Acoustic depth gauges measure the surface height changes that result from a combination of precipitation, post-depositional drift, sublimation/melt and compaction (Steffen and others, 1996). Data from the CP AWS span May 1995 to the present, with some discontinuities due to intermittent equipment failures.

Precipitation data were gathered from four meteorological stations in west central Greenland. Three of these stations are located in complex topography along the coast, while Kangerlussuaq is situated in a more protected embayment slightly further inland (Fig. 1). Complete annual precipitation data begin for most of the stations at about 1960, with the exception of Ilulissat, which extends back to 1874. For these stations, greater precipitation occurs in summer and autumn and minimum precipitation in spring. For Aasiaat and Sisimiut, precipitation exhibits an increasing trend for all seasons, especially in the most recent decade (Mernild and others, 2014). The precipitation data from the three coastal stations do not agree with the inland CP A_n (Fig. 3); however, Kangerlussuaq precipitation agrees well despite its greater distance from the CP site. This agreement likely reflects its more inland location, which may be more representative of the ice sheet than the other coastal stations. Data from the AWS and CP ice core overlap for 11 complete years (1996–2006); however, aggregating the sub-hourly AWS surface height changes to annual accumulation is difficult because of some large data gaps from instrument failure. In years with missing data, AWS accumulation may be spuriously low (e.g. 1998, 1999, 2002 and 2003). Nevertheless, the AWS and CP ice core generally agree (Fig. 4). Unfortunately, there are no long-term precipitation records over the ice sheet, so simulated data must be used to determine whether seasonal biases exist in accumulation. The reanalysis and regional climate model data described below will be tested against the in situ AWS and CP accumulation at monthly and annual timescales, respectively.

Simulated accumulation is derived from the reanalyses and regional model using two distinct methods that yield accumulated snow depth and/or precipitation minus evaporation ($P - E$). Accumulated snow depth from the gridded reanalyses is most comparable with AWS surface height

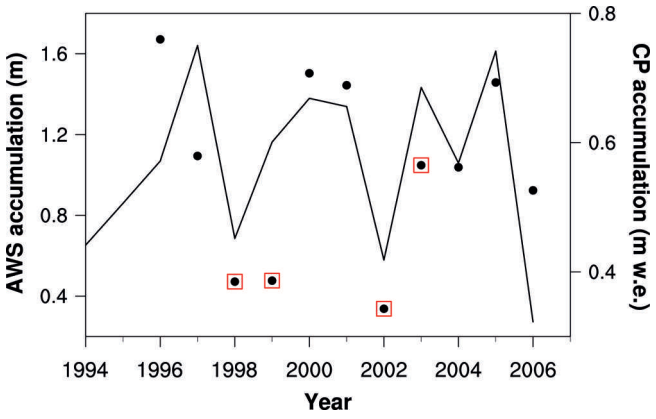

Fig. 4. Annual AWS accumulation (circles) and annual accumulation from the CP ice core (line); AWS observations with missing data are enclosed in red boxes.

data; however, several reanalyses exhibit major issues with this variable. The NCEP/NCAR (US National Centers for Environmental Prediction/US National Center for Atmospheric Research) reanalysis (NCEP1) has well-known problems with scaling of the snow depth parameter (Kanamitsu and others, 2002). ECMWF (European Centre for Medium-Range Weather Forecasts) Re-analysis (ERA-40) and ERA-Interim (ERA-I) nudge the snow depth parameter to climatology (Betts and others, 2003; Dee and others 2011), which distorts the accumulation. Fortunately, the NCEP/DOE (US Department of Energy) II (NCEP2) and the 20th Century Reanalysis (20CR) more accurately represent snow depth and are used for this study. For snow analysis, NCEP2 only ingests weekly snow cover derived from satellite images over the Northern Hemisphere, and provides model estimates of snow depth in w.e. (Kanamitsu and others, 2002). 20CR only assimilates surface pressure observations with prescribed sea surface temperatures to generate gridded model output (Compo and others, 2011). Thus, both of these reanalyzed variables are independent of the CP AWS data. This study examines the snow depth parameters from the 2° gridcell in 20CR (Compo and others, 2011) and the 2.5° gridcell in NCEP2 (Kanamitsu and others, 2002) corresponding to the CP site. Neighboring gridcells in the reanalysis data were also investigated since the CP site is located near the edge of its gridcell. The cells to the east exhibit similar variability in daily snow depth but, as expected, different overall magnitudes due to various gridcell characteristics (e.g. elevation, latitude). The adjacent gridcell to the west was more representative of the ablation zone of the GrIS as the snow depth parameter exhibited a steady decline. Only results from the corresponding gridcell are presented here as these are most relevant to the AWS site; however, it will be shown that CP accumulation contains a large-scale climate signal.

Reanalysis datasets are also used to define the lateral boundary conditions for regional-scale models such as the Modèle Atmosphérique Régional (MAR). Daily MAR output is available online for the GrIS from 1958 to 2013 (Tedesco and others, 2013). The development of MAR is explained by Gallée and Schayes (1994), and its configuration for the GrIS is described by Fettweis (2007). MAR runs at 25 km horizontal resolution, and its boundary conditions are driven by ERA-40 and ERA-I (Tedesco and others, 2013). MAR has previously been used to explore surface mass balance over the GrIS (Rae and others, 2012; Vernon and others, 2013). Among other regional-scale models, MAR performs best for Greenland surface mass balance below 1500 m a.s.l.; however, above 1500 m MAR overestimates accumulation (Vernon and others, 2013). Rae and others (2012) suggest that regional-scale models with detailed snow schemes, such as MAR, tend to provide more accurate representations of Greenland surface mass balance than models without detailed snow physics.

The AWS and simulated snow depth data were aggregated monthly using two techniques. First, the average monthly snow depth was calculated by averaging the daily snow depth for each month. NCEP2 expresses snow depth in m w.e., 20CR contains two snow depth variables reported in m (snow) and m w.e., and the AWS and MAR express snow depth in m (snow). MAR also simulates snow density, which is used in this study to convert daily changes in MAR snow height (i.e. accumulation) into snow height in m w.e. In this study, variables expressing snow depth in m (snow) and m w.e. are represented by SD_m and SD_{we}, respectively. Snowpack depth was adjusted for model recalibrations every 5 years for 20CR and every 1 year for MAR; adjustment was not necessary for NCEP2 as there appeared to be no recalibrations. The second aggregation technique involves the calculation of snow-depth-derived accumulation determined using the daily change in snow height (ΔSH), which was summed for each month. Similar to the snow depth, variables expressing changes in surface height in m (snow) and m w.e. are represented by ΔSH_m and ΔSH_{we}, respectively. The terms snow depth and snow height are used interchangeably in this study; however, to clarify the abbreviations, depth is used for accumulated depth while height is used for accumulation (i.e. changes in depth/surface height).

The snow depth variables are most easily compared with the AWS observations of snow height; however, there are other methods of calculating accumulation ($P - E$). For the reanalysis datasets that contain unsuitable snow depth variables (NCEP1, ERA-40 and ERA-I), $P - E$ can be used to calculate accumulation for comparison with the AWS accumulation determined from snow height changes. $P - E$ may not be fully representative of snow height changes because it does not include factors such as melt, runoff, compaction and/or drift. Precipitation also includes both snowfall and rainfall. Rainfall would not be discernible in the AWS observations as it would not add to snow height. For NCEP1, NCEP2 and 20CR, precipitation cannot be separated into snowfall and rainfall, but for MAR, ERA-40 and ERA-I these variables are separate. Comparisons were made between $P - E$ and $S - E$ (snowfall minus evaporation); rainfall is virtually insignificant for the CP site. Evaporation was determined using the surface latent heat flux and the latent heat of vaporization at 0°C ($L_v = 2.501 \times 10^{-6}$). Similar to some of the snow depth variables, $P - E$ is expressed in m w.e. ($P - E_{we}$). Table 1 summarizes the reanalysis and model products used in this study.

RESULTS

Seasonal accumulation variability

The monthly SD_m from the AWS observations and simulated SD_m and SD_{we} from MAR, 20CR and NCEP2 for 1995–2006 are shown in Figure 5. The magnitude of the simulated snow depth variables depends on when the model runs begin,

similar to how the AWS snow height observations are initialized to zero upon installation. Thus, for direct comparison with the observations, the simulated snow depth is set to zero in June 1995, for which the first complete month of observational data is available after the AWS was installed at CP in May 1995.

All observations and simulations indicate that prior to 2007 CP was situated well within the accumulation zone of the ice sheet as the snow depth increases over the observational period. MAR and 20CR SD_m underestimate the overall increase in snow height due to their overestimation of summer surface lowering (Fig. 5a). Hanna and others (2011) found similar results, with too much evaporation over the GrIS in 20CR. Seasonal variations are more prevalent in the simulated data than observed by the AWS. The rate of snow depth increase is difficult to compare between AWS SD_m and simulated SD_{we}, which requires knowledge of the snow density. The exaggerated seasonality does not appear in the NCEP2 SD_{we} (Fig. 5b), which unfortunately reaches a preset maximum threshold at about 2004, after which snow height can no longer increase. Although the threshold is an issue with the post-2004 NCEP2 SD_{we}, for 1995–2004 NCEP2 SD_{we} outperforms the other simulated data. The SD_m (Fig. 5a) and SD_{we} (Fig. 5b) derived from MAR differ greatly, likely reflecting an error in the snow density variable.

The 1995–2004 correlations between the observed (AWS) and simulated monthly snow depths all exceed 0.8 (Table 2), and NCEP2 slightly outperforms the others. These high correlation coefficients partially reflect the increasing nature of all these variables. Linearly detrending each variable better elucidates the intra- and interannual variability (not shown). As expected, the correlations for the detrended data are lower but still significant ($p < 0.003$). The detrended r values for MAR and 20CR versus the observations range from 0.30 to 0.63 for both SD_m and SD_{we}, while the NCEP2 SD_{we} r value is 0.87 (Table 2). Since these variables are accumulated data there is an inherent autocorrelation, which explains the high correlation coefficients.

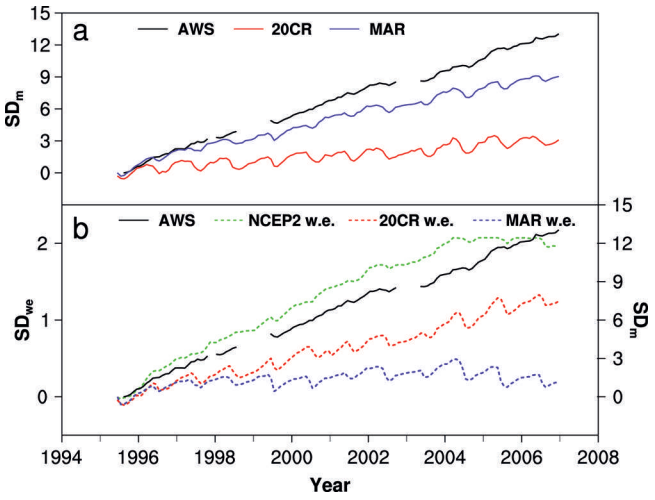

Fig. 5. (a) SD_m from the AWS (black), 20CR (red) and MAR (purple) and (b) SD_{we} from NCEP2 (dashed green), 20CR (dashed red) and MAR (dashed purple) for the CP site.

The snow-depth-derived accumulation records (ΔSH_m and ΔSH_{we}) for the observations (AWS), reanalyses and regional model are similar, as expected given the strong relationship among the snow depth variables. Both ΔSH_m and ΔSH_{we} from MAR and 20CR exaggerate the surface lowering during summer, which is not observed by the AWS. NCEP2 ΔSH_{we} does not overestimate the surface lowering and hence best represents the observations at this site. Correlations between ΔSH_m from the AWS and ΔSH_m and ΔSH_{we} from MAR and 20CR (not detrended) range from 0.34 to 0.49, while that for ΔSH_{we} from NCEP2 gives an r value of 0.71 (Table 2). These results are surprising as NCEP2 has the coarsest resolution (2.5°) compared with 20CR (2.0°) and MAR (25 km). Correlations for the monthly accumulated $P - E_{we}$ variables with the AWS ΔSH_m are very similar among the datasets and range from $r = 0.47$ for

Table 1. Characteristics of reanalysis datasets and the regional model

	NCEP1	NCEP2	20CR	ERA-40	ERA-I	MAR
Time	1948–2006	1979–2006	1871–2006	1957–2002	1979–2006	1958–2006
Resolution	2.5°	2.5°	2.0°	2.5°	0.75°	25 km
Variables	$P - E_{we}$	$P - E_{we}$, SD_{we}	$P - E_{we}$, SD_{we}, SD_m	$P - E_{we}$	$P - E_{we}$	$P - E_{we}$, SD_{we}, SD_m

Table 2. Correlation coefficients between monthly AWS SD_m and simulated SD_{we} (SD_m) and between monthly AWS ΔSH_m and simulated ΔSH_{we} (ΔSH_m) and $P - E_{we}$. All correlations are significant at the 99% confidence level

		NCEP1	NCEP2	20CR	MAR	ERA-40	ERA-I
AWS SD_m	SD_{we} (SD_m)		1995–2004	1995–2004	1995–2004		
			0.999	0.981 (0.874)	0.813 (0.994)		
	Detrended SD_{we} (SD_m)		1995–2004	1995–2004	1995–2004		
			0.868	0.389 (0.304)	0.414 (0.631)		
AWS ΔSH_m	ΔSH_{we} (ΔSH_m)		1995–2004	1995–2004	1995–2004		
			0.709	0.496 (0.424)	0.340 (0.378)		
	$P - E_{we}$	1995–2006	1995–2006	1995–2006	1995–2006	1995–2002	1995–2006
		0.575	0.568	0.472	0.513	0.589	0.611

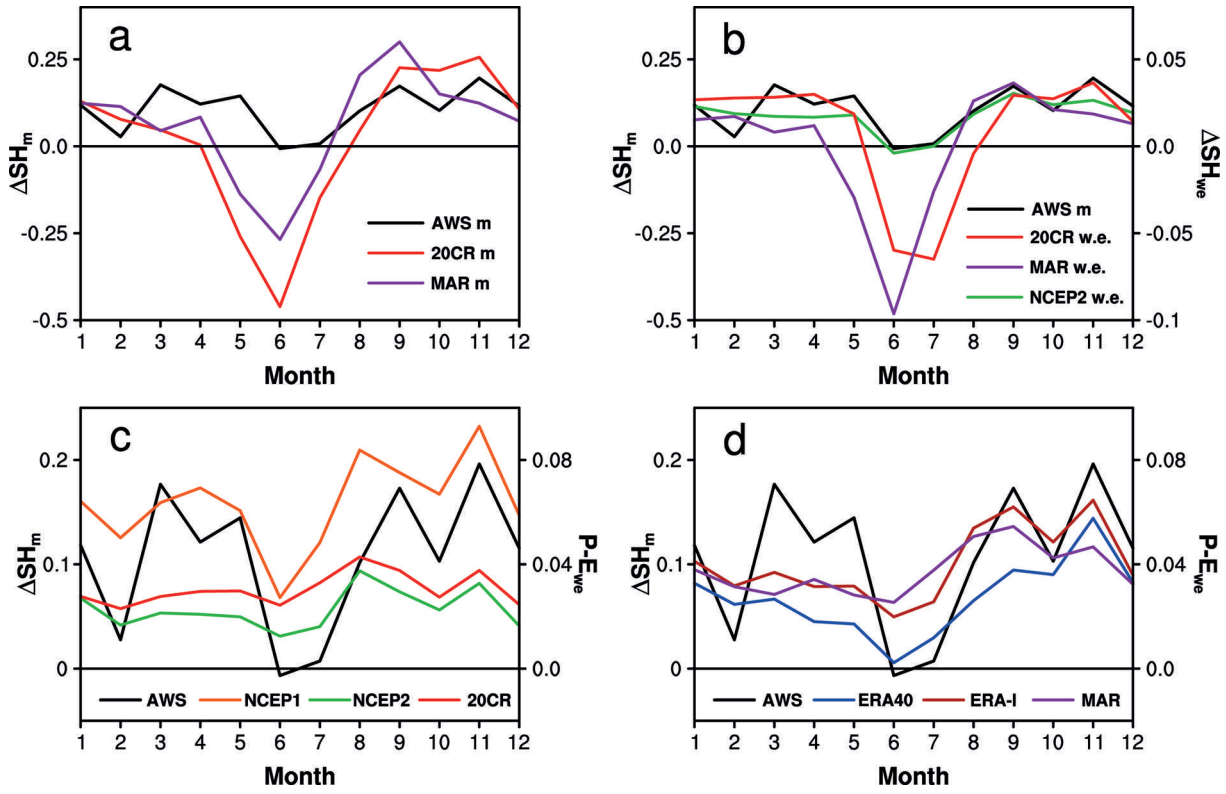

Fig. 6. Post-1995 mean monthly accumulation from AWS observations (black), 20CR (red), MAR (purple), NCEP1 (orange), NCEP2 (green), ERA-40 (blue) and ERA-I (brown) for (a) ΔSH_m, (b) ΔSH_{we} and (c, d) $P - E_{we}$ for the CP site.

20CR to $r = 0.61$ for ERA-I (Table 2). All correlations are significant at the 99% level. Nevertheless, the NCEP2 ΔSH_{we} still performs best at the monthly timescale.

As the simulated accumulation data agree well with the AWS observations, they can be used to characterize the seasonal distribution of accumulation at the CP site. For 1995–2006, the AWS mean monthly ΔSH_m shows maximum accumulation in autumn and spring and minimum accumulation in summer, with a slight surface lowering (i.e. negative accumulation) in June (Fig. 6a). The ΔSH_m from 20CR and MAR clearly exaggerates surface lowering in the summer, as does their corresponding ΔSH_{we} variable (Fig. 6b). These 20CR and MAR variables suggest that ~40–90% of the total annual accumulation is removed by summer ablation which, if true, would negatively influence the ability of the CP ice core to preserve a robust climate history. Clearly, this is not the case as the AWS observations indicate that ablation only removes <1% of the annual accumulation. This result is bolstered by the NCEP2 ΔSH_{we} which is very similar to the AWS ΔSH_m. Although the AWS observations are in m and NCEP2 data are in m w.e., the zero accumulation line is the same, and NCEP2 ΔSH_{we} also shows a similar slight surface lowering in June (Fig. 6b). The simulated mean monthly $P - E_{we}$ shows similar patterns to the AWS ΔSH_m with a maximum in autumn and a minimum in summer (Fig. 6c and d). NCEP1 $P - E_{we}$ shows considerably higher accumulation than the other datasets. $P - E_{we}$ from MAR and ERA-I are very similar as the MAR boundary conditions are driven by ERA-I during this time.

None of the accumulation records shows a summer maximum in accumulation, indicating that if a summer precipitation maximum exists it is offset by surface lowering, likely from increased melt and/or sublimation. Owing to the short AWS record, this analysis covers only 1995–2006, during which warming over Greenland has become more pronounced (Hanna and others, 2008). To explore whether this pattern of summer surface lowering is a recent phenomenon, the reanalysis and model datasets that extend into the pre-1995 conditions can be examined to determine whether summer surface lowering was prevalent prior to 1995. Figure 7 shows the mean monthly accumulation for all the simulated accumulation variables. All the variables show a less-pronounced summer minimum prior to 1995, although the pre- and post-1995 difference is greater for some variables than others. The ΔSH_m and ΔSH_{we} from 20CR and MAR still show considerable surface lowering in the summer months (Fig. 7a and b). The NCEP2 ΔSH_{we}, which showed slight lowering in summer for the post-1995 period, shows positive accumulation throughout the year (Fig. 7b) for the full simulation period (post-1979), although summer accumulation is still less than autumn and spring accumulation, similar to the post-1995 period. The $P - E_{we}$ accumulation for NCEP1 (Fig. 7c) shows a less pronounced summer minimum than in the post-1995 period, but $P - E_{we}$ from NCEP2 and 20CR shows very little difference between the periods. ERA-40 and ERA-I $P - E_{we}$ show much more muted summer minima in the pre-1995 period (Fig. 7d). MAR data remain similar to those from ERA-40 and ERA-I as these reanalyses define the MAR boundary conditions before and after 1979, respectively. Accumulation peaks in late summer and autumn for many of the variables; however, for most, the late-summer and autumn accumulation does not greatly exceed that of winter. These simulated accumulation records confirm the lack of a summer bias in accumulation at the CP site even though the summer lowering is more pronounced since 1995. The CP ice-core-derived A_n may be slightly biased toward the

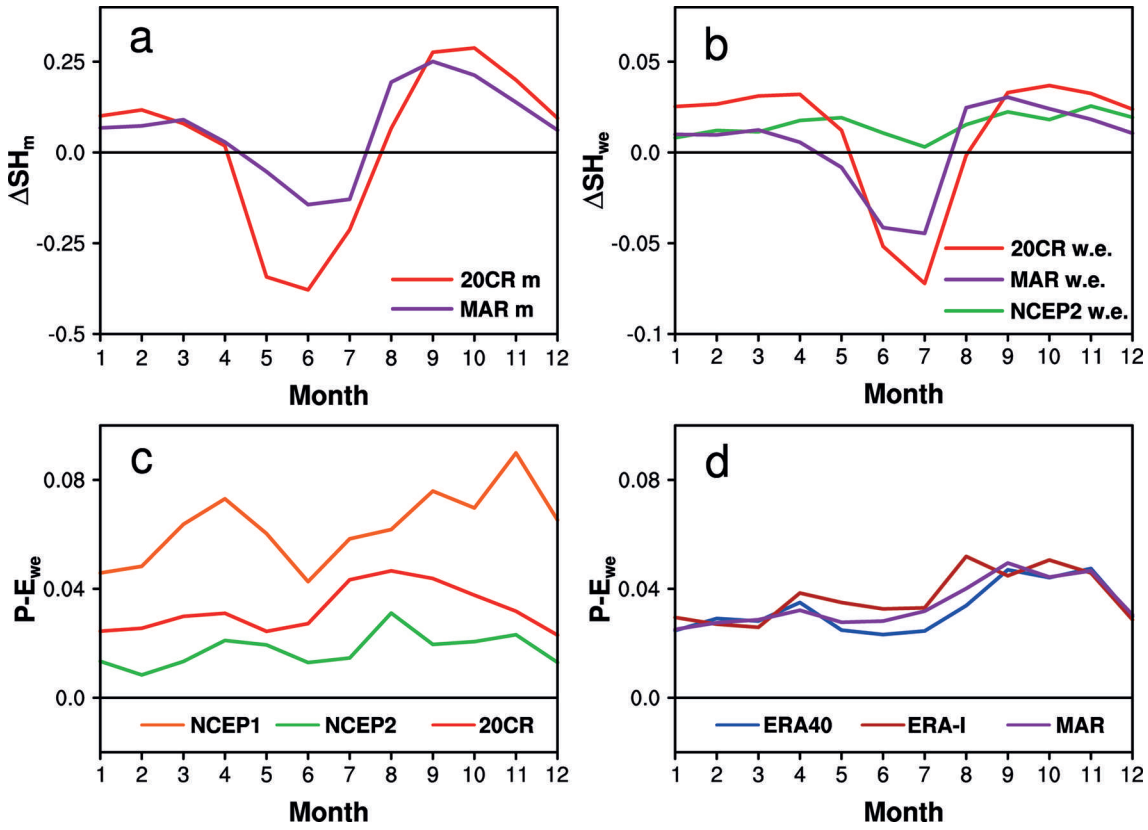

Fig. 7. Same as Figure 6, but for the entire simulated periods (see Table 1 for time periods).

autumn as most of the simulated data show higher autumn accumulation both before and after 1995.

Annual accumulation variability

Comparing the CP ice-core-derived A_n and accumulation derived from the reanalyses and the model for the CP site confirms that both represent the annual signal well. Figure 8 shows the annual accumulation variables (ΔSH_m ΔSH_{we} and $P - E_{we}$) with the CP A_n record. The simulated accumulation records clearly capture the interannual variability. Virtually all correlation coefficients among the accumulation variables (Table 3) are significant at the 99% confidence level. MAR ΔSH_{we} is the exception and, as previously mentioned, this likely reflects snow density errors. Variability in MAR $P - E_{we}$ is most closely related to variability in A_n from the CP ice core ($r = 0.66$). Differences in magnitude between the in situ and simulated accumulation are not surprising as gridcell areal data are compared with a single point measurement (i.e. the CP ice core). Most of the datasets underestimate accumulation relative to that from the CP core. NCEP1 $P - E_{we}$ data are the exception (Fig. 8c) and this result is similar to that of Chen and others (2011) who found that NCEP1 overestimated precipitation over the GrIS. Accumulation values derived from ΔSH_m cannot be compared directly with the CP ice core A_n since they are in different units (Fig. 8a). The ΔSH_{we} variables underestimate accumulation (Fig. 8b) more so than $P - E_{we}$ (Fig. 8c and d), although NCEP2 ΔSH_{we} is closer in

Table 3. Correlation coefficients between CP ice-core-derived A_n (m w.e.) and simulated ΔSH_{we}, ΔSH_m and $P - E_{we}$

	Period	Snow depth variable				
		NCEP2 ΔSH_{we}	20CR ΔSH_m	20CR ΔSH_{we}	MAR ΔSH_m	MAR ΔSH_{we}
CP annual accumulation	1979–2004	0.547	0.565	0.551	0.627	0.299*
	1958–2004		0.524	0.541	0.562	0.302*
	1871–2004		0.343	0.360		

		$P - E_{we}$					
		NCEP1	NCEP2	20CR	ERA-40†	ERA-I	MAR
CP annual accumulation	1979–2006	0.598	0.652	0.661	0.676	0.754	0.771
	1958–2006	0.468		0.549	0.594		0.662
	1871–2006			0.350			

*Not significant at the 99% level. †Limited to 2002.

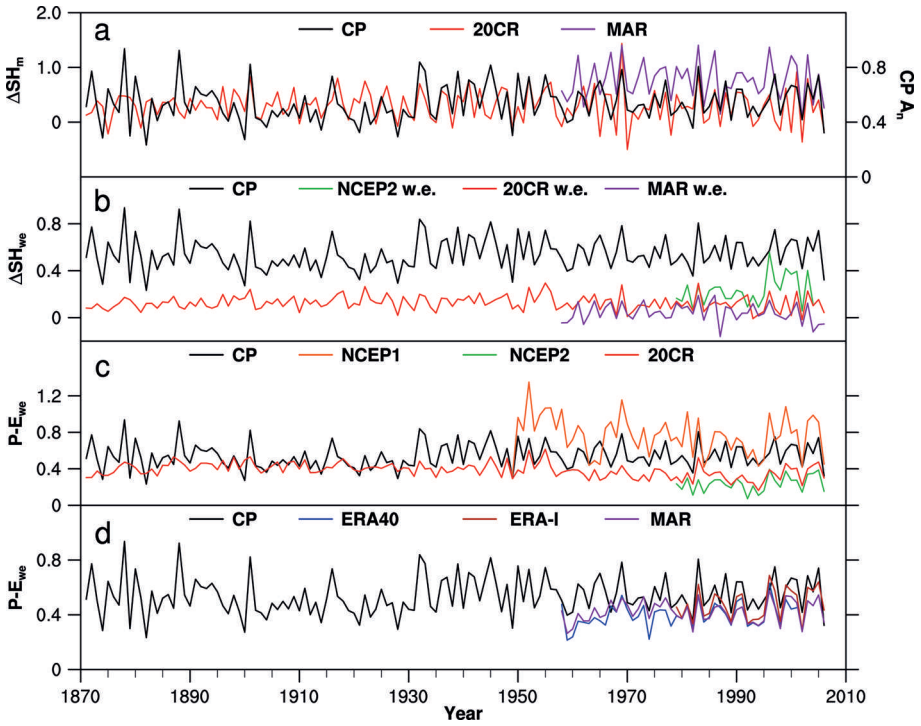

Fig. 8. CP ice-core-derived A_n (black) compared with annual simulated (a) ΔSH_m, (b) ΔSH_{we} and (c) $P - E_{we}$ for 20CR (red), NCEP2 (green) and NCEP1 (orange) and (d) $P - E_{we}$ for ERA-40 (blue), ERA-I (brown) and MAR (purple) for the CP site.

magnitude to CP A_n than ΔSH_{we} from MAR or 20CR. NCEP1 $P - E_{we}$ overestimates accumulation, while NCEP2 $P - E_{we}$ underestimates accumulation. The 20CR $P - E_{we}$ is close in magnitude to CP A_n, but the difference increases after 1960 when 20CR accumulation exhibits a slight decreasing trend (Fig. 8c). $P - E_{we}$ from ERA-40, ERA-I and MAR most closely captures the magnitude of accumulation after 1960 (Fig. 8d). MAR is not independent of ERA-40 or ERA-I, although it is more highly correlated with the CP A_n. Chen and others (2011) found that among NCEP1, NCEP2, ERA-40 and ERA-I, only $P - E_{we}$ from ERA-I was able to accurately represent accumulation over West Greenland. Since MAR has a higher resolution and is laterally defined by ERA-I, its higher accuracy is not surprising. Correlations between CP A_n and simulated seasonal accumulation time series were also calculated (not shown), but generally the correlation coefficients were stronger among the annual time series, which indicates that CP A_n is an annual signal and not biased by any particular season.

At the CP site, the reanalyzed and modeled accumulation compare well with the in situ observations, and demonstrate the ability of both the gridded and point data to capture both sub-annual and interannual variability. This is surprising as the AWS and ice-core-derived accumulation are susceptible to local post-depositional effects, such as surface erosion and redeposition during snowdrifting. On the other end of the spectrum, most of the gridded fields are relatively low-resolution. The agreement among these records indicates the strong potential and feasibility in the upscaling representation of in situ accumulation and also the downscaling representation of the interpolated gridded accumulation.

The accumulation records from reanalyses and the AWS observations do not support a strong seasonal bias in net annual accumulation at the CP site. Thus the proxy records derived from the CP ice core should represent the annual climate variability without a discernible seasonal bias. One of the objectives for the CP ice core is to investigate the history of the NAO, which is primarily a winter phenomenon. Spatial correlations between CP A_n and gridded annual mean sea-level pressure (MSLP) from ERA-I reveal the classic NAO structure, with positive correlations in the vicinity of the Icelandic low and negative correlations with the subtropical Azores high (Fig. 9). This analysis was repeated for seasonal MSLP (not shown), but the correlations are strongest for the annual timescale, indicating that CP accumulation is truly an annual signal. Thus, the annually resolved ice-core record from the west central Greenland site at CP is suitable for future investigations of large-scale climate variability, such as the NAO.

CONCLUSIONS

An ice core retrieved from CP in west central Greenland and extending back to AD 1766 with annual resolution affords the opportunity to investigate long-term changes in the major climate drivers of that region, including the NAO. The NAO is generally a wintertime phenomenon, and previous modeling studies as well as coastal precipitation records have suggested that west central Greenland receives more accumulation in the summer. This implies that proxy data from ice cores in this region may be biased toward climate conditions in summer. Modeling studies tend to analyze west central Greenland as one large region, although the dynamics on the topographically complex coast are likely to be quite different from those at higher inland sites. The ice-core-derived A_n must adequately represent the winter climate to capture winter variability in the NAO, and thus it is important to confirm or refute the presence of a summer accumulation bias.

Surface height data from an AWS installed at CP in the mid-1990s reveal that the greatest increases in surface height (i.e. net accumulation) do not occur in summer. This

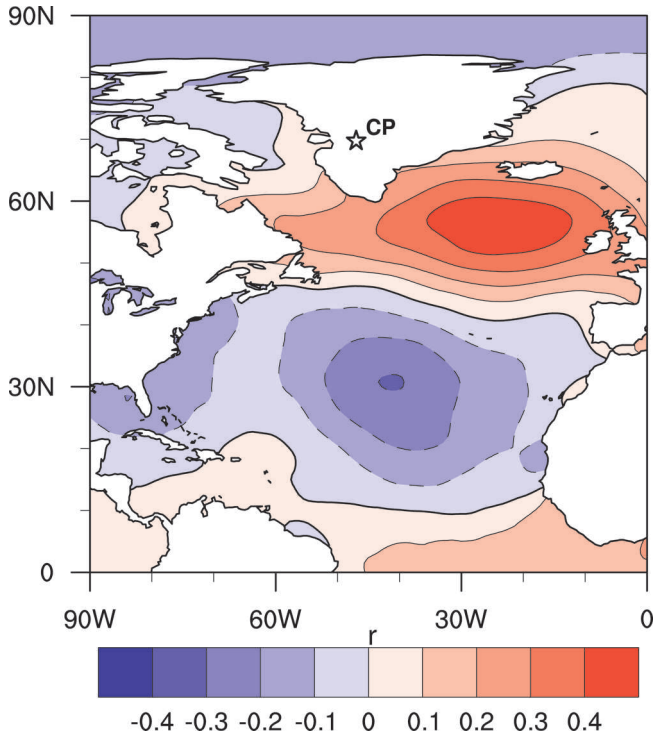

Fig. 9. Spatial correlations between the CP ice-core-derived A_n and annual mean sea-level pressure from ERA-I for 1979–2006.

indicates that either there is not a precipitation maximum in summer or that the precipitation maximum is being offset by other processes such as melt, sublimation and/or compaction that lower the ice-sheet surface. The monthly AWS record compares well with the accumulated snow depth from both the NCEP2 and 20CR reanalyses and the regional MAR model, although agreement is best with the NCEP2 data. The simulated accumulation records support the AWS-derived summer minimum in accumulation in the post-1995 period (Fig. 6) and demonstrate that although summer minima are more pronounced after 1995, prior to installation of the AWS in 1995, summer accumulation does not exceed that in other seasons (Fig. 7). The annual changes in simulated accumulation and A_n from the CP ice core all agree well, demonstrating the strength of each record to reasonably represent the net accumulation of this region and their potential in further analysis of west central Greenland's climate history. The snowpack variables (ΔSH_m and ΔSH_{we}) and $P - E_{we}$ from reanalyses and the MAR regional model provide a simple technique for investigating the seasonality of accumulation at other locations in the accumulation zone of the ice sheet, although ideally this should be tested against AWS acoustic depth gauge measurements. The records from the CP site indicate no summer bias in accumulation and a modest autumn bias in accumulation. They demonstrate that west central Greenland ice cores are appropriate for reconstructions of climate variability and winter circulation patterns including the NAO. Future work with the CP ice-core record will investigate the past influence of the NAO over west central Greenland.

ACKNOWLEDGEMENTS

This work was supported by NAGS-5032 (US National Science Foundation (NSF)–CReSIS) and The Ohio State University's Climate, Water and Carbon Program. We thank Jason Box and Konrad Steffen for providing the AWS snow height data. We acknowledge David Bromwich for thoughtful discussion and insight and thank two anonymous reviewers whose suggestions greatly improved the paper. The NCEP1, NCEP2 and 20CR data are available online (http://www.esrl.noaa.gov/psd/) from the US National Oceanic and Atmospheric Administration (NOAA) and the Earth System Research Laboratory's (ESRL) Physical Sciences Division (PSD). ERA-40 and ERA-I data are from the European Centre for Medium-Range Weather Forecasts (ECMWF) data server (http://apps.ecmwf.int/datasets/). This is Byrd Polar and Climate Research Center contribution No.1437.

REFERENCES

Aðalgeirsdóttir G and 7 others (2009) *Assessment of the temperature, precipitation and snow in the RCM HIRHAM4 at 25 km resolution*. (from Danish Climate Centre Report 09–08) Danish Meteorological Institute, Copenhagen

Appenzeller C, Schwander J, Sommer S and Stocker TF (1998) The North Atlantic Oscillation and its imprint on precipitation and ice accumulation in Greenland. *Geophys. Res. Lett.*, **25**(11), 1939–1942 (doi: 10.1029/98GL01227)

Betts AK, Ball JH and Viterbo P (2003) Evaluation of the ERA-40 surface water budget and surface temperature for the Mackenzie River basin. *J. Hydromet.*, **4**(6), 1194–1211 (doi: 10.1175/1525-7541(2003)004<1194:EOTESW>2.0.CO;2)

Bromwich DH, Chen QS, Li Y and Cullather RI (1999) Precipitation over Greenland and its relation to the North Atlantic Oscillation. *J. Geophys. Res.*, **104**(D18), 22 103–22 115 (doi: 10.1029/1999JD900373)

Calder CA, Craigmile PF and Mosley-Thompson E (2008) Spatial variation in the influence of the North Atlantic Oscillation on precipitation across Greenland. *J. Geophys. Res.*, **113**(D6), D06112 (doi: 10.1029/2007JD009227)

Chen L, Johannessen OM, Wang H and Ohmura A (2011) Accumulation over the Greenland Ice Sheet as represented in reanalysis data. *Adv. Atmos. Sci.*, **28**(5), 1030–1038 (doi: 10.1007/s00376- 010-0150-9)

Chen QS, Bromwich DH and Bai L (1997) Precipitation over Greenland retrieved by a dynamic method and its relation to cyclonic activity. *J. Climate*, **10**(5), 839–870 (doi: 10.1175/1520-0442(1997)010<0839:POGRBA>2.0.CO;2)

Compo GP and 26 others (2011) The Twentieth Century Reanalysis Project. *Q. J. R. Meteorol. Soc.*, **137**(654), 1–28 (doi: 10.1002/qj.776)

Dee DP and 35 others (2011) The ERA-Interim reanalysis: configuration and performance of the data assimilation system. *Q. J. R. Meteorol. Soc.*, **137**(656), 553–597 (doi: 10.1002/qj.828)

Fettweis X (2007) Reconstruction of the 1979–2006 Greenland ice sheet surface mass balance using the regional climate model MAR. *Cryosphere*, **1**(1), 21–40 (doi: 10.5194/tc-1-21-2007)

Gallée H and Schayes G (1994) Development of a three-dimensional meso-γ primitive equation model: katabatic winds simulation in the area of Terra Nova Bay, Antarctica. *Mon. Weather Rev.*, **122**(4), 671–685 (doi: 10.1175/1520-0493(1994)122<0671:DOATDM>2.0.CO;2)

Hanna E and 8 others (2008) Increased runoff from melt from the Greenland Ice Sheet: a response to global warming. *J. Climate*, **21**(2), 331–341 (doi: 10.1175/2007JCLI1964.1)

Hanna E and 12 others (2011) Greenland Ice Sheet surface mass balance 1870 to 2010 based on Twentieth Century Reanalysis, and links with global climate forcing. *J. Geophys. Res.*, **116**(D24), D24121 (doi: 10.1029/2011JD016387)

Kanamitsu M and 6 others (2002) NCEP-DOE AMIP-II Reanalysis (R-2). *Bull. Am. Meteorol. Soc.*, **83**(11), 1631–1643

Mernild SH and 9 others (2014) Greenland precipitation trends in a long-term instrumental climate context (1890–2012): evaluation of coastal and ice core records. *Int. J. Climatol.* (doi: 10.1002/joc.3986)

Merz N, Raible CC, Fischer H, Varma V, Prange M and Stocker TF (2013) Greenland accumulation and its connection to the large-scale atmospheric circulation in ERA-Interim and paleoclimate simulations. *Climate Past*, **9**(6), 2433–2450 (doi: 10.5194/cp-9-2433-2013)

Mosley-Thompson E and 8 others (2001) Local- to regional-scale variability of annual net accumulation on the Greenland ice sheet from PARCA cores. *J. Geophys. Res.*, **106**(D24), 33 839–33 851 (doi: 10.1029/2001JD900067)

Mosley-Thompson ES, Readinger CR, Craigmile P, Thompson LG and Calder CA (2005) Regional sensitivity of Greenland precipitation to NAO variability. *Geophys. Res. Lett.*, **32**(24), L24707 (doi: 10.1029/2005GL024776)

Porter SE (2013) Assessing whether climate variability in the Pacific Basin influences the climate over the North Atlantic and Greenland and modulates sea ice extent. (PhD thesis, Ohio State University) http://rave.ohiolink.edu/etdc/view?acc_num=osu1366297907

Rae JGL and 14 others (2012) Greenland ice sheet surface mass balance: evaluating simulations and making projections with regional climate models. *Cryosphere*, **6**(6), 1275–1294 (doi: 10.5194/tc-6-1275-2012)

Schuenemann KC, Cassano JJ and Finnis J (2009) Synoptic forcing of precipitation over Greenland: climatology for 1961–99. *J. Hydromet.*, **10**(1), 60–78 (doi: 10.1175/2008JHM1014.1)

Steffen K and Box J (2001) Surface climatology of the Greenland ice sheet: Greenland Climate Network 1995–1999. *J. Geophys. Res.*, **106**(D24), 33 951–33 964 (doi: 10.1029/2001JD900161)

Steffen K, Box J and Abdalati W (1996) Greenland climate network: GC-net. *CRREL Spec. Rep.* 96-27, 98–103

Tedesco M, Fettweis X, Alexander P, Green G and Datta T (2013) *MAR Greenland outputs 1958–2012, ver. 3.2*. CCNY Digital Archive http://www.cryocity.org/mar-explorer.html

Thomas RH and PARCA I (2001) Program for Arctic Regional Climate Assessment (PARCA): goals, key findings, and future directions. *J. Geophys. Res.*, **106**(D24), 33 691–33 705 (doi: 10.1029/2001JD900042)

Vernon CL and 6 others (2013) Surface mass balance model intercomparison for the Greenland ice sheet. *Cryosphere*, **7**(2), 599–614 (doi: 10.5194/tc-7-599-2013)

MS received 18 December 2013 and accepted in revised form 8 August 2014